



## Estimation of Slip Distribution of the 2007 Bengkulu Earthquake from GPS Observations Using the Least-Squares Inversion Method

Moehammad Awaluddin<sup>1,2</sup>, Irwan Meilano<sup>2</sup> & Sri Widiyantoro<sup>3</sup>

<sup>1</sup>Geodetic Engineering, Faculty of Engineering, University of Diponegoro,  
Jl. Prof. Soedharto Tembalang, Semarang, Jawa Timur 50255, Indonesia

<sup>2</sup>Geodesy Research Division, Faculty of Earth Science and Technology,

Institut Teknologi Bandung, Jl. Ganesha, 10 Bandung, Jawa Barat 40132, Indonesia

<sup>3</sup>Global Geophysics Research Division, Faculty of Mining and Petroleum Engineering,  
Institut Teknologi Bandung, Jl. Ganesha 10, Bandung, Jawa Barat 40132, Indonesia

Email: awal210874@yahoo.com

**Abstract.** Continuous Global Positioning System (GPS) observations showed significant crustal displacements as a result of the Bengkulu earthquake occurring on September 12, 2007. A maximum horizontal displacement of 2.11 m was observed at PRKB station, while the vertical component at BSAT station was lifted up with a maximum of 0.73 m, and the vertical component at LAIS station had subsided -0.97 m. Adding more constraints on the inversion for the Bengkulu earthquake slip distribution inferred from GPS observations can help solve the underdetermined least-squares inversion. Checkerboard tests were performed to help conduct the weighting for constraining the inversion. The inversion calculation yielded an optimal value for the slip distribution by giving the smoothing constraint a weight of 0.001 and the slip constraint a weight of = 0 at the edge of the earthquake rupture area. The maximum co-seismic slip of the optimal inversion calculation was 5.12 m at the lower area of PRKB station and BSAT station. The seismic moment calculated from the optimal slip distribution was  $7.14 \times 10^{21}$  Nm, which is equivalent to a magnitude of 8.5.

**Keywords:** *Bengkulu earthquake; GPS data; least-squares inversion; slip distribution.*

### 1 Introduction

Bengkulu is one of the areas in Southwest Sumatra, Indonesia, which has been deformed by subduction activity. Due to its location close to the subduction zone of the Indo-Australian oceanic plate beneath the Eurasian plate, this area is prone to earthquakes. It is recorded in the history of seismicity on the western coast of Sumatra that earthquakes with a large magnitude have occurred in Bengkulu in 1833 (magnitude 8.7), in 2000 (magnitude 7.9) and most recently on 12 September 2007, with a main earthquake magnitude of 8.5 at a depth of 34 km. Several other large earthquakes followed this earthquake on the same day, with a maximum magnitude of 7.9 [1].

---

Received March 21<sup>st</sup>, 2012, Revised July 26<sup>th</sup>, 2012, Accepted for publication July 27<sup>th</sup>, 2012.

Copyright © 2012 Published by LPPM ITB & PII, ISSN: 1978-3051, DOI: 10.5614/itbj.eng.sci.2012.44.2.6

GPS is a satellite navigation system that determines position based on satellite observation. In recent years GPS techniques have been applied repeatedly for slip rate estimations of active faults in Indonesia. Meilano, *et al.* [2] used campaign and continuous GPS data to make a preliminary estimation of the slip rate of the Lembang fault. The results of these GPS measurements suggest that the Lembang fault has a shallow creeping portion and a deeper locking portion. Using GPS-based geodetic surveys, Prawirodirdjo, *et al.* [3] revealed deformation above the Sumatra subduction zone that shows nearly complete coupling of the forearc to the subduction plate south of  $0.5^{\circ}\text{S}$  and half as much to the north. Abidin, *et al.* [4] used GPS survey methods to study the inter-seismic deformation of three active faults in West Java (*i.e.* the Cimandiri, Lembang and Baribis faults), and the co-seismic and post-seismic deformation related to the May 2006 Yogyakarta and the July 2006 South Java earthquakes.

Elastic dislocation theory assumes that the crust of the earth is homogeneous, isotropic, linear and elastic [5]. Displacement at an earthquake field will result in a displacement of the earth's surface. The magnitude of the displacement cannot be measured directly, but with the data of the displacements on the earth's surface that can be obtained from GPS measurements, the displacement can be calculated using an inversion of the surface displacement data [5]. However, the resulting solution is commonly not unique or stable. Thus, several inversion techniques, exploiting the linear nature of the problem and involving several kinds of constraints of geophysical and geological parameters, are required to obtain a unique and stable solution [6].

Several studies calculating the slip distribution associated with the Bengkulu earthquake in 2007 have been conducted, by USGS [7], Gusman, *et al.* [8] and Ambikapathy, *et al.* [9]. USGS calculated the slip distribution using teleseismic data and a relatively small-sized earthquake rupture area of  $20\text{ km} \times 14.5\text{ km}$  [7]. Gusman, *et al.* [8] used the data of tsunami waves and InSAR, while Ambikapathy, *et al.* [9] used a relatively large earthquake area based on the Sumatran GPS Array (SuGAR) data. In these studies, none has used least-square inversion calculation on a relatively small earthquake area and data obtained from (near-field) GPS measurements. This paper calculates the slip distribution of the earthquake area using the SuGAR measurement data and the least-squares inversion technique, as well as constraints of geophysical and geological parameters, thus obtaining an optimal slip distribution solution for the 2007 Bengkulu earthquake.

## **2      2007 Bengkulu Earthquake**

The 2007 Bengkulu earthquake had its epicenter at coordinates  $4.520^{\circ}\text{S}$ ,  $101.374^{\circ}\text{E}$  at a depth of 34 km [1]. The earthquake occurred as a result of fault

slip on the boundary between the Indo-Australian and Eurasian plates. Around the location of the earthquake, the Indo-Australian plate moves N-NE towards the SE Eurasian plate at a speed of approximately 60 mm/year. The direction of the relative plate motion is oblique to the orientation of the offshore plate boundary along the west coast of Sumatra. The component of the plate movement is perpendicular to the boundaries and is accommodated by the faulting force on the offshore plate boundaries. Most of the plate motion components are parallel to the plate boundary and are accommodated by strike-slip faulting of the Sumatra fault on the mainland [1].

The seismic moment yielded by the 2007 Bengkulu earthquake according to USGS was  $5.05 \times 10^{21}$  Nm (equivalent to  $M_w = 8.4$ ). Meanwhile, the moment magnitude yielded by USGS from the seismic data was 8.5 and the obtained maximum slip was 4 m [7]. Gusman, *et al.* [8] performed an inversion calculation of the slip distribution using the data of tsunami waves and InSAR. They divided the earthquake field into 72 discrete units with a size of 25 km x 25 km. The result of the inversion calculation carried out by Gusman, *et al.* [8] produced slip distributions that indicate a maximum value of  $\pm 6$  m at two discrete locations. The seismic moment generated by the Bengkulu earthquake according to Gusman, *et al.* [8] was  $3.8 \times 10^{21}$  Nm (equivalent to  $M_w = 8.3$ ).

Ambikapathy, *et al.* [9] also conducted a calculation of the 2007 Bengkulu earthquake slip distribution using the SuGAR data, and obtained a maximum slip of 7 m. They calculated seven discrete earthquake fields, which is larger compared to those used by USGS and Gusman, *et al.* [8]. The results of the slip among the discrete units were not smooth. Ambikapathy, *et al.* [9] did not calculate the seismic moment of the resulting slip distribution.

Of the three studies, USGS [7] and Gusman, *et al.* [8] have used smaller discrete field sizes than Ambikapathy, *et al.* [9]. Only USGS [7] has calculated the larger area of the earthquake field, up to the edge of the trench. Assuming that the earthquake field experienced continuous ruptures but its slip values were not homogeneous, the resulting slip distribution is expected to be more appropriate to the actual physical phenomena if a smaller discrete unit size is used.

The data used by USGS were categorized as far-field data (observed from a distance), thereby making them relatively less sensitive than the GPS observation data (SuGAR) used by Ambikapathy, *et al.* [9] or the tsunami wave and InSAR data used by Gusman, *et al.* [8] in capturing the phenomena of the earthquake field slip.

In this study a least-squares inversion of the slip distribution data is performed, using the near-field SuGAR data and treating the earthquake field as a collection of small-size discrete areas. The global CMT solution was used to calculate the seismic moment and moment magnitude of the Bengkulu earthquake [10]. The result was  $6.71 \times 10^{21}$  Nm, which is equivalent to  $M_w = 8.5$ .

### 3 Least Squares Inversion

With the linear relationship between the data ( $d$ ) and the model parameters ( $m$ ), the calculation of the inversion can be performed using the following procedure:

$$d = G.m \quad (1)$$

with  $G$  as a common modeling function that relates the model to quantities in the data domain. In other words, function  $G$  allows us to predict the data for a particular model  $m$  [11].

One of the commonly used inversion techniques is the least-squares calculation method. The application of least-squares inversion is used to estimate model  $m$ , having a response (calculated data) that matches the field data. Therefore, the minimum mean square error (least-square) criterion is re-applied to obtain the solution for model  $m$  [12].

The parameters for model  $m$  can be calculated by least-squares inversion with the following equation [11]:

$$m = (G^T G)^{-1} G^T d \quad (2)$$

If the calculation of the inversion uses some weights, Eq. (2) becomes:

$$m = (G^T W_e G)^{-1} G^T W_e d \quad (3)$$

$W_e$  serves as the weight matrix and T is the transpose matrix.

An elastic dislocation formula can be used to calculate the displacement of the points on the surface, if the values of the dip-slip and strike-slip are known [5, 13]. According to the elastic dislocation formula, the values of the displacement on the surface are directly proportional to the values of the strike-slip, dip-slip and opening in a linear manner. By utilizing the properties of the linearity of the equation that connects the displacement in the field of the earthquake to the displacement of the points on the surface, matrix  $G$  can be constructed. In Eq. (1), vector  $m$  is the model parameter to be searched. In this case,  $m$  is the strike-slip and dip-slip of the earthquake field, and matrix  $d$  consists of the vectors of the displacement of the points on the surface.

By making the value of the slip equal to one scaling unit, the displacement of the point on the surface can be calculated. If the slip value equals  $n$  times the scaling unit, with a linear relationship, the value of the surface point displacement equals  $n \times G_0$ . Such an assumption leads to matrix  $G$  by calculating the point displacement on the surface, inserting the slip value as equal to one scaling unit. Hereafter, matrix  $G$  is called the basis matrix.

The slips in the earthquake rupture area have a spatial variation of model parameters that is not too high in terms of the inversion calculation. The difference with the adjacent model parameter values is minimized through smoothing. One of the matrix smoothing models ( $MS$ ) that can be used to smooth the least squares inversion solution can be seen in the following  $MS$  matrix [11].

$$MS = \begin{pmatrix} 1 & -2 & 1 & 0 & \dots & \dots & 0 \\ 0 & 1 & -2 & 1 & 0 & \dots & \vdots \\ \vdots & \dots & \dots & \dots & \dots & \dots & \vdots \\ \vdots & \dots & 0 & 1 & -2 & 1 & 0 \\ 0 & \dots & \dots & 0 & 1 & -2 & 1 \end{pmatrix} \quad (4)$$

Another constraint used in this study is to give the slip at the edges of the earthquake slip area a discrete value = 0. If this constraint is added to the inversion calculation, Eq. (1) will be:

$$\begin{pmatrix} G_{Hor} \\ G_{Ver} \\ P3.S \\ P4.T \end{pmatrix} \cdot m = \begin{pmatrix} P1.d_{Hor} \\ P2.d_{Ver} \\ 0 \\ 0 \end{pmatrix} \quad (5)$$

- P1 = weight for horizontal measurement data
- P2 = weight for vertical measurement data
- P3 = weight for smoothing constraint
- P4 = weight for constraint of slip value = zero at the edges of the discrete earthquake field
- $G_{Hor}$  = basis matrix for horizontal measurement data
- $G_{Ver}$  = basis matrix for vertical measurement data
- $d_{Hor}$  = horizontal measurement data
- $d_{Ver}$  = vertical measurement data
- S = basis matrix for smoothing constraint
- T = basis matrix for constraint of slip value = zero at the edges of the discrete earthquake field

#### 4 Earthquake Source Model

The model parameters of the earthquake source used in the calculation are:

1. Earthquake rupture area geometry consisting of long ( $L$ ) = 68900 m, width ( $W$ ) = 183324 m, coordinates of the upper midpoint of the earthquake field ( $\lambda, \phi$ ) = ( $100.228^\circ, -3.904^\circ$ ), strike ( $\alpha$ ) =  $141.719^\circ$ , dip ( $\delta$ ) =  $-13.097^\circ$  and depth ( $D$  = 5000 m);
2. Strike-slip (ss) and dip-slip (ds) as the parameters that will be estimated, and the opening = 0;

One approach to the problem of earthquake slip distribution inversion is to divide the earthquake field into several uniform discrete units, so that the number of known slips is smaller than the number of data. The unknown slips are then estimated using the least-squares method. The weakness of this approach is that the specific discrete field geometry may not provide adequate spatial representation of the various fault slips due to faults being discretized very roughly, or a discrete unit size that is still too large. In order to estimate the continuous distribution of slip, the discrete units must be relatively small. In general, this means that the number of model parameters will increase and may exceed the number of data. In that case, the equation system becomes ill-posed (*i.e.*, the system is underdetermined and the solution is not unique) [6]. Thus, in order to find a particular solution, constraints must be added to the equation system.

In this study, the earthquake rupture area is made up of  $30 \times 10$  discrete units, and therefore there are 300 slip planes. Each plane of the earthquake has two parameters (strike-slip and dip-slip), giving a total number of 600 parameters.

#### 5 Co-seismic Displacement from GPS Observations

The SuGAR data used in this study are data from 2006, 2007 and 2008, and the number of GPS stations is 13. The dual-frequency carrier phase and pseudo-range observations were processed using Bernese GPS Processing Software version 5.0 by Hugentobler, *et al.* [14], developed at the University of Bern. The precise ephemerides and earth rotation parameters from the International GNSS Service (IGS) were used and the coordinate reference system was established by connecting to the nearby IGS stations. Integer biases were fixed with the quasi-ionosphere free (QIF) algorithm. All relevant geodynamic reductions were applied in order to enable a careful determination of crustal deformation. Ocean tidal loading was considered using the GOT00 model by Bos and Scherneck [15]. The results of the SuGAR data processing were the daily coordinates for each SuGAR station. The topocentric coordinates on the first day of each station served as the origin of the topocentric coordinate

system of each respective station, hence each station had its own topocentric coordinate system.

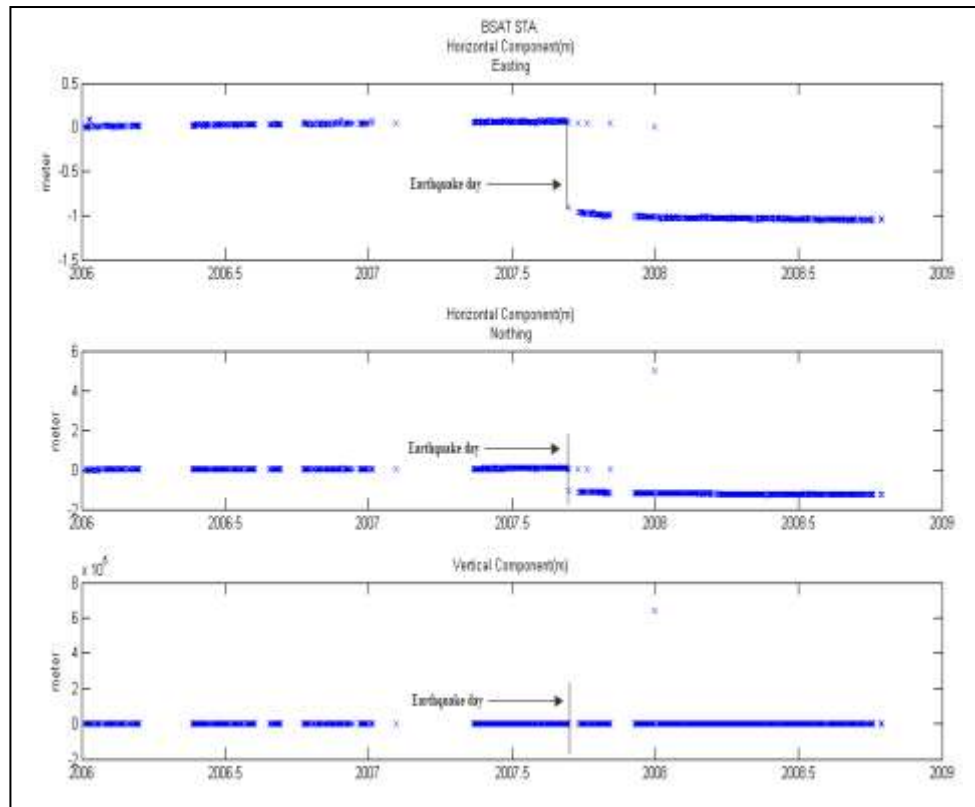


**Figure 1** Daily coordinates of BSAT station from 2006 – 2009.

From the time series (Figures 1 and 2) and the topocentric coordinates of each SuGAR station (Table 1), ten data were taken before the earthquake (including data on the day of the earthquake) and ten data after the earthquake. Then the average values and standard deviation of each ten data were calculated. If the deviation between the data and the average value exceeded one standard deviation, the coordinate data were rejected. The difference between the average values of the accepted data before and after the earthquake is the displacement vector due to earthquake co-seismic deformation as shown in Table 1 and Figure 3.

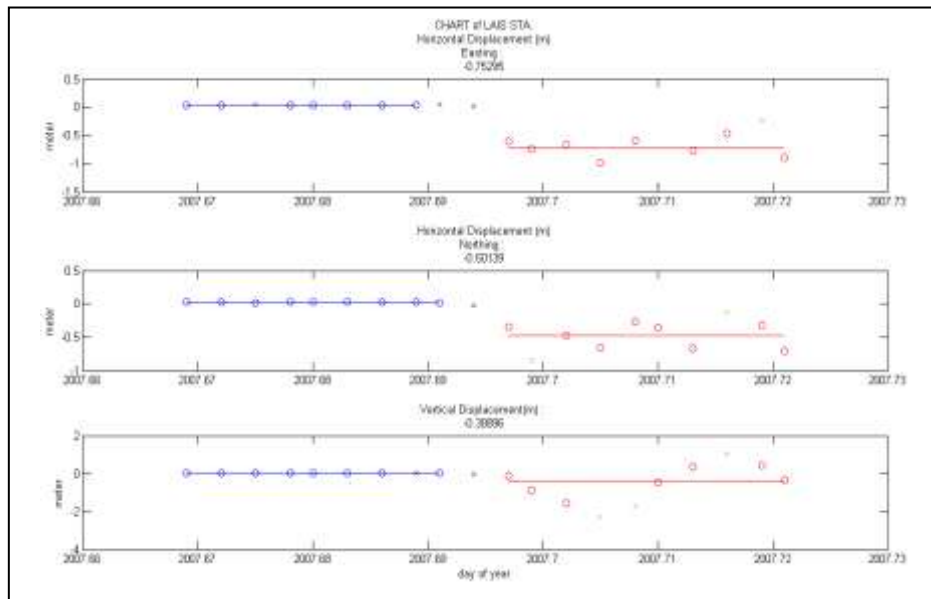


**Figure 2** Calculation results of displacement vector of LAIS station.

**Table 1** Displacement vectors of SuGA stations due to co-seismic deformation of the Bengkulu earthquake.

STA	Displacement (m)			Standard Deviation (m)		
	EW	NS	UD	EW	NS	UD
BSAT	-1.029	-1.174	0.728	0.014	0.015	0.006
BTET	-0.015	0.013	-0.004	0.004	0.004	0.003
JMBI	-0.080	-0.054	-0.001	0.005	0.007	0.006
LAIS	-0.753	-0.501	-0.389	0.088	0.090	0.357
LNNG	-0.477	-0.575	-0.165	0.082	0.110	0.241
MKMK	-0.578	-0.709	-0.204	0.016	0.018	0.010
MLKN	0.026	-0.009	-0.033	0.005	0.003	0.008
MNNA	-0.072	-0.002	-0.016	0.005	0.003	0.007
MSAI	-0.008	0.034	-0.002	0.005	0.007	0.004
NGNG	-0.103	-0.035	0.023	0.048	0.001	0.017
PPNJ	-0.486	-0.571	0.257	0.010	0.007	0.011
PRKB	-1.252	-1.701	-0.318	0.102	0.103	0.279
PSKI	-0.126	-0.227	-0.040	0.003	0.001	0.005



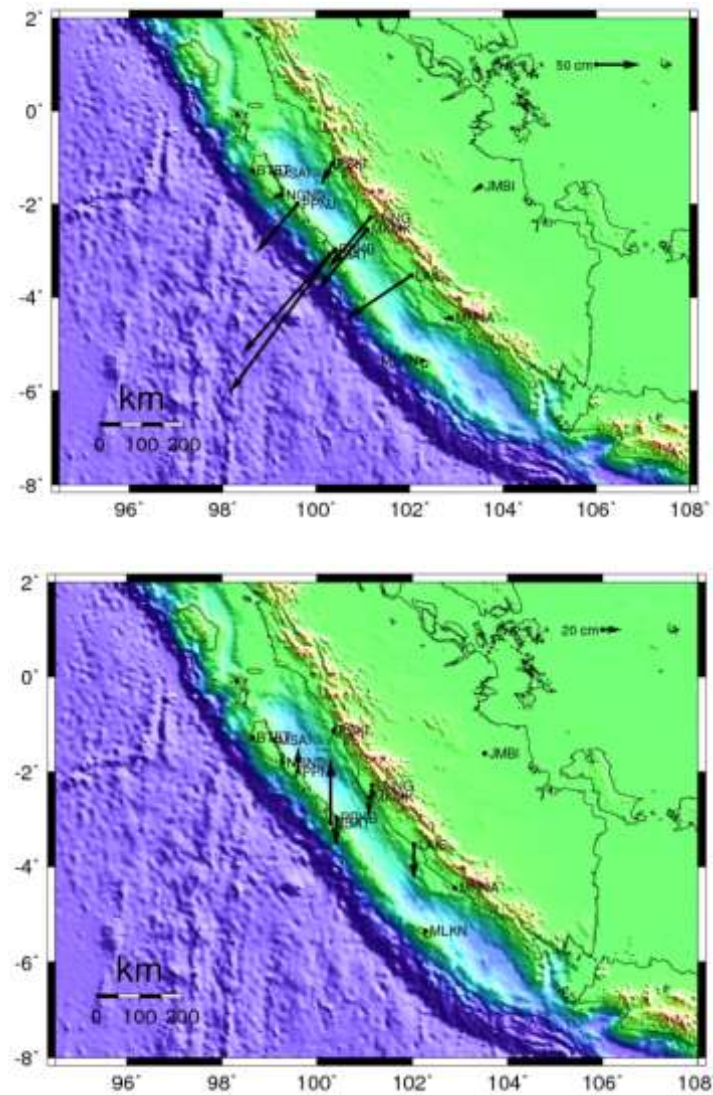


**Figure 1** Displacement vectors of GPS SuGAR stations (upper panel: horizontal displacement, lower panel: vertical displacement).

## 6 Least-Squares Inversion Calculation

Input data for the calculation were a discrete model of the earthquake plane, the coordinates of the observation points and the displacement vectors of the SuGAR points. The parameters to be estimated for each discrete earthquake field unit are strike-slip and dip-slip. If calculation of slip distribution is performed

for  $(m \times n)$  discrete earthquake field units, the number of parameters to be estimated is  $2 \times (m \times n)$ .

The dip-slip basis matrix was constructed by performing a forward calculation of displacement of (number of observation points  $k$ ) SuGAR points for each discrete field of the model by setting a value of dip-slip = 1 and strike-slip = 0 for each dip-slip basis matrix component. The result of the forward calculation was  $(3 \times k)$  displacement data. Thus, for the discrete earthquake field with a size of  $m \times n$  units and a number of SuGAR points  $k$ , a basis matrix for dip-slip was obtained with a size of  $(3 \times k)$  rows and  $(m \times n)$  columns. The strike-slip basis matrix was made in the same manner, but using dip-slip = 0 and strike-slip = 1. Subsequently, the dip-slip basis matrix and strike-slip matrix were combined to form matrix  $G$ , with a size of  $(3 \times k)$  rows and  $2 \times (m \times n)$  columns. The constraints used in this study were a smoothing constraint and a slip constraint with value = 0 at the edges of the earthquake area.

The smoothing constraint matrix for  $(m \times n)$  discrete field units regarded the dip-slip and strike-slip. The size of the matrix is  $(2 \times (((m - 2) \times n) + ((n - 2) \times m)))$  rows and  $(2 \times (m \times n))$  columns. The matrix for slip constraint = zero, at the edges of the discrete earthquake field, has a size of  $((2 \times m) + (2 \times (n - 2)))$  rows and  $(2 \times (m \times n))$  columns for the values of dip-slip and strike-slip.

The  $d$  column matrix, with a size of  $(3 \times k)$ , was constructed from the displacement data of the SuGAR points. In the calculation process, basis matrix  $G$  was combined with the constraint matrix. To the  $d$  column matrix a value of 0 was added for as many times as the number of rows of the constraint matrix.

The weight matrix is structured as a diagonal matrix with the size of the number of rows of matrix  $G$  plus the number of rows of the constraint matrix. The diagonal elements are the weight values of the horizontal and vertical displacement data and the constraint weight used.

From the results of the calculation, the values of the dip-slip and strike-slip parameters for each discrete field can be obtained. These parameters can be incorporated in the model of the earthquake area to perform a forward calculation of the displacement of all points on the surface.

## 6.1 Checkerboard Test

A checkerboard test (CBT) was conducted to determine the appropriate weighting for the observation equation of the basis and constraint matrices. The CBT was performed using the synthetic data resulting from the forward calculation.

Checkerboard tests were carried out using various weightings, *i.e.* weights for horizontal observation data ( $P1$ ), weights for vertical observation data ( $P2$ ), weights for the smoothing constraint ( $P3$ ) and weights for the slip constraint with value zero at the edge of the earthquake area ( $P4$ ).

The synthetic models were made by taking a dip-slip value of  $-5$  m and a strike-slip value of  $0$  m in the first 3 parts, and a dip-slip value of  $0$  m and a strike-slip value of  $0$  m in the other 3 parts, as shown in Figure 4. The black-colored vectors indicate displacements on the surface resulting from the forward calculation of the synthetic model. The orange-colored vectors are the synthetic dip-slip values.

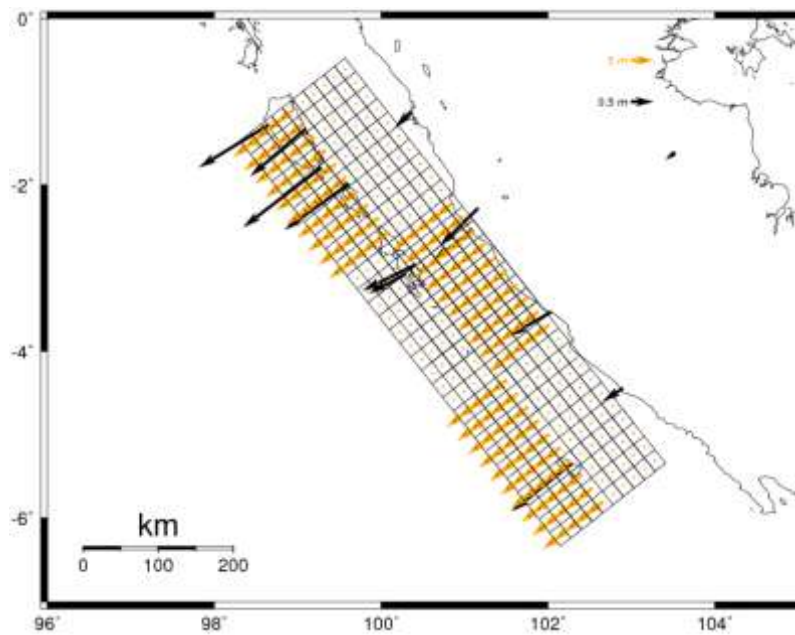


**Figure 2** Discrete synthetic model 30 x 10.

The weighting variations have been conducted for  $P3$  and  $P4$ , while for  $P1$  the weight was determined = 1 and  $P2 = 0.1$ . There were 12 weights for  $P3$  and  $P4$ . Each weight value of  $P3$  was paired alternately with 12 weights of  $P4$ ; thus, 144 possible variations of weights  $P3$  and  $P4$  were obtained. The test results of RMS1 and RMS2 yielded a minimum RMS value on the weight pair of  $P3 = 0.005$  and  $P4 = 0.0001$ .

In the next step, an inversion calculation was performed with three variations of weights, chosen as follows:

1.  $P1=1, P2=0.3, P3=0.005$  and  $P4=0.0001$
2.  $P1=1, P2=0.3, P3=0.005$  and  $P4=0.0005$
3.  $P1=1, P2=0.3, P3=0.001$  and  $P4=0.0001$

## 6.2 Inversion using SuGAr Data Weight Combination 1

In this model the maximum value of the slip is 3.74 m (figures 5 and 6). The slip direction inclines toward the trench, which indicates that the dip-slip is more dominant than the strike-slip, except at the southeast and northwest edges. The slip value is highest around the lower parts of PRKB and BSAT station, and tends to decline toward the edges of the earthquake field.

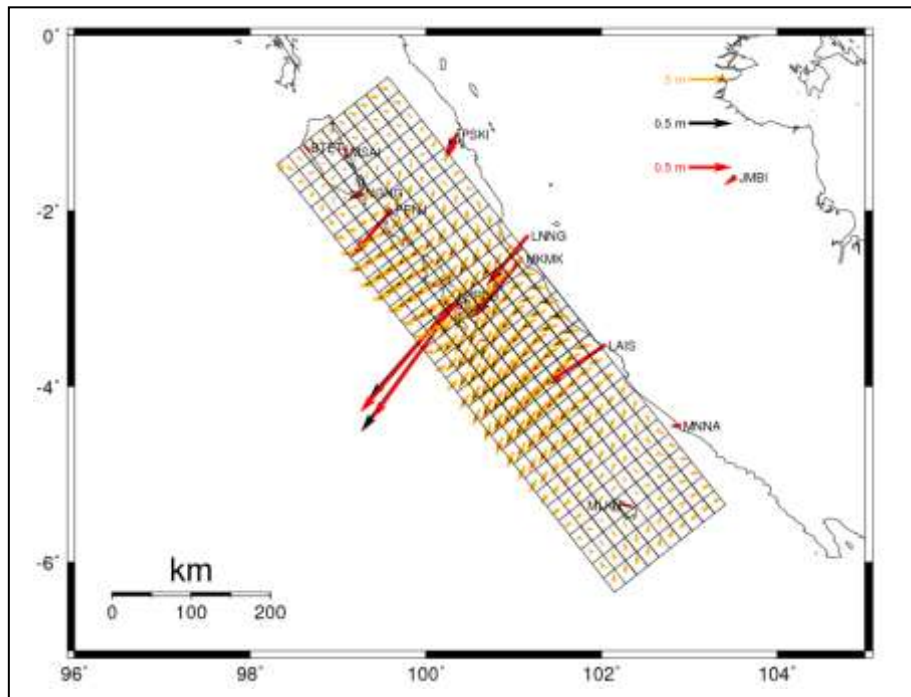


**Figure 3** Slip distribution as a result of the inversion of SuGAr data for 30 x 10 discrete field units with weight combination 1 (black vectors are the vectors of each point's displacement using SuGAr data; red vectors are the model's displacement vectors; orange vectors are the slip yielded from the inversion of discrete-field data).

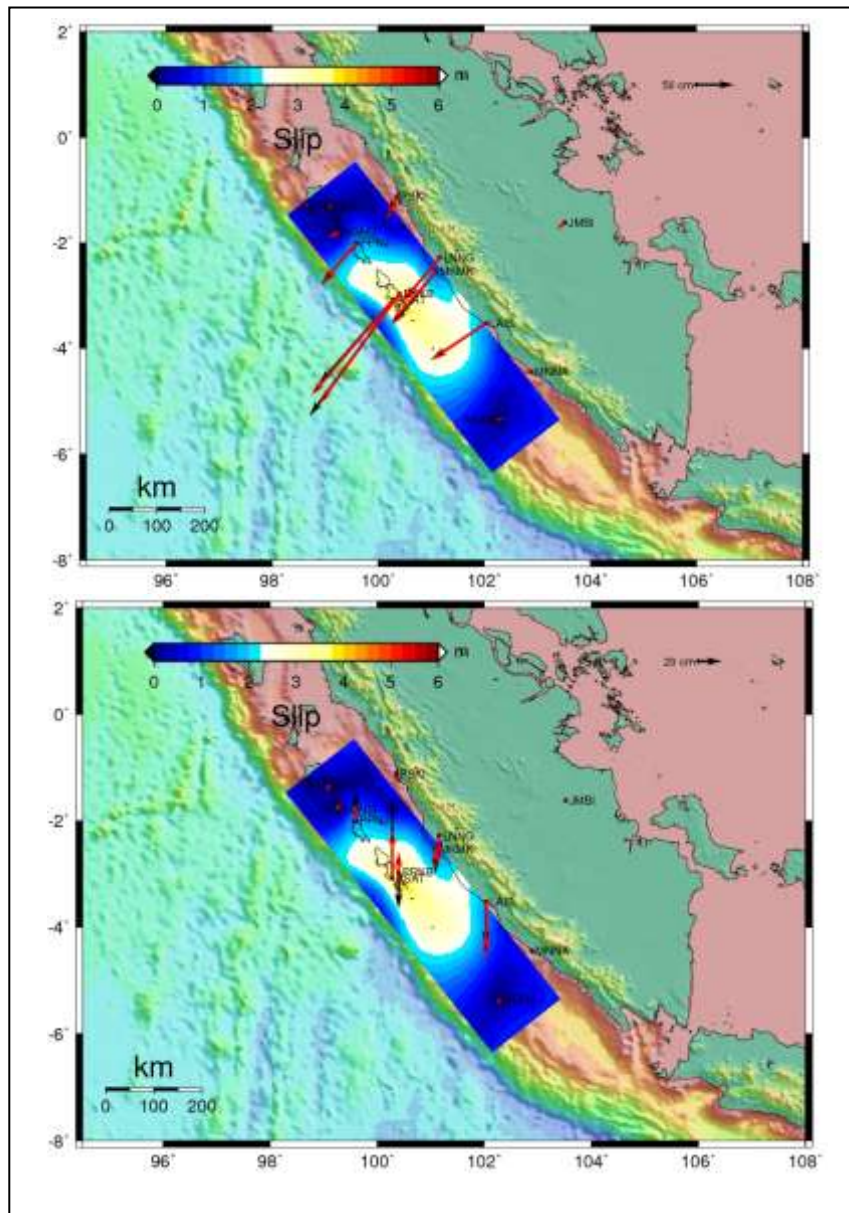


**Figure 4** Contour of the slip distribution resulting from the inversion of SuGAR data for 30 x 10 discrete field units with weight combination 1 (the upper image is the horizontal component, the lower image is the vertical component, the black vectors are the vectors of each point's displacement using SuGAR data, the red vectors are the model's displacements vectors).

### 6.3 Inversion Using SuGAr Data Weight Combination 2

Here, the maximum slip value is 3.95 m (Figures 7 and 8). The slip direction also inclines toward the trench, showing that the dip-slip is more dominant than the strike-slip, except in the discrete southeast and northwest edges. The slip value is highest around the lower parts of PRKB and BSAT station, and tends to decline toward the edges of the earthquake field.

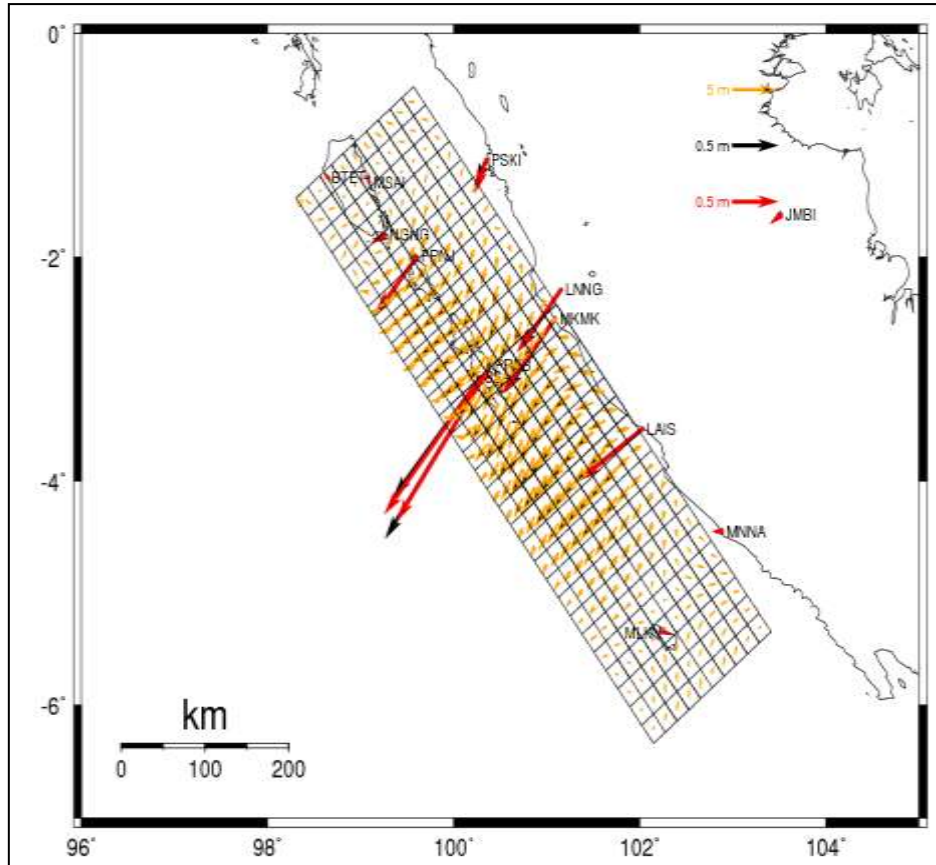


**Figure 5** Slip distribution as a result of the inversion of SuGAr data for 30 x 10 discrete fields with weight combination 2 (black vectors depict the vector of each point's displacement using SuGAr data, red vectors are the model's displacement vectors; orange vectors are the slip yielded from the inversion of discrete-field data).



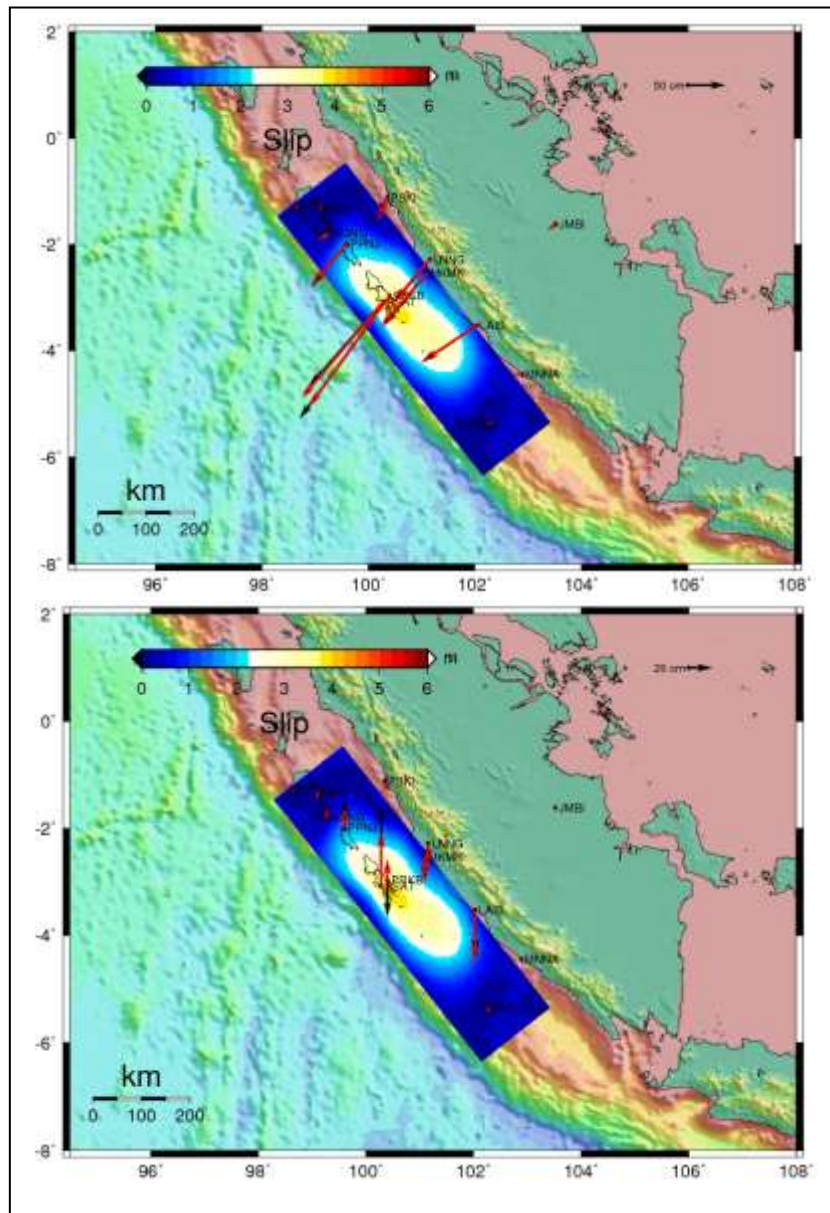


**Figure 6** Contour of the slip distribution resulting from the inversion of SuGAR data for  $30 \times 10$  discrete field units with weight combination 2 (the upper image is the horizontal component, the lower image is the vertical component, the black vectors are the vectors of each point's displacement using SuGAR data, the red vectors are the model's displacements vectors).

#### 6.4 Inversion Using SuGAR Data Weight Combination 3

By using combination 3, the maximum slip value is 5.12 m (figures 9 and 10). The slip direction also inclines toward the trench, which shows that the dip-slip is more dominant than the strike-slip, except in the southeast and northwest edges. The slip value is highest around the lower parts of PRKB station and BSAT station, and tends to decline toward the edges of the earthquake field.

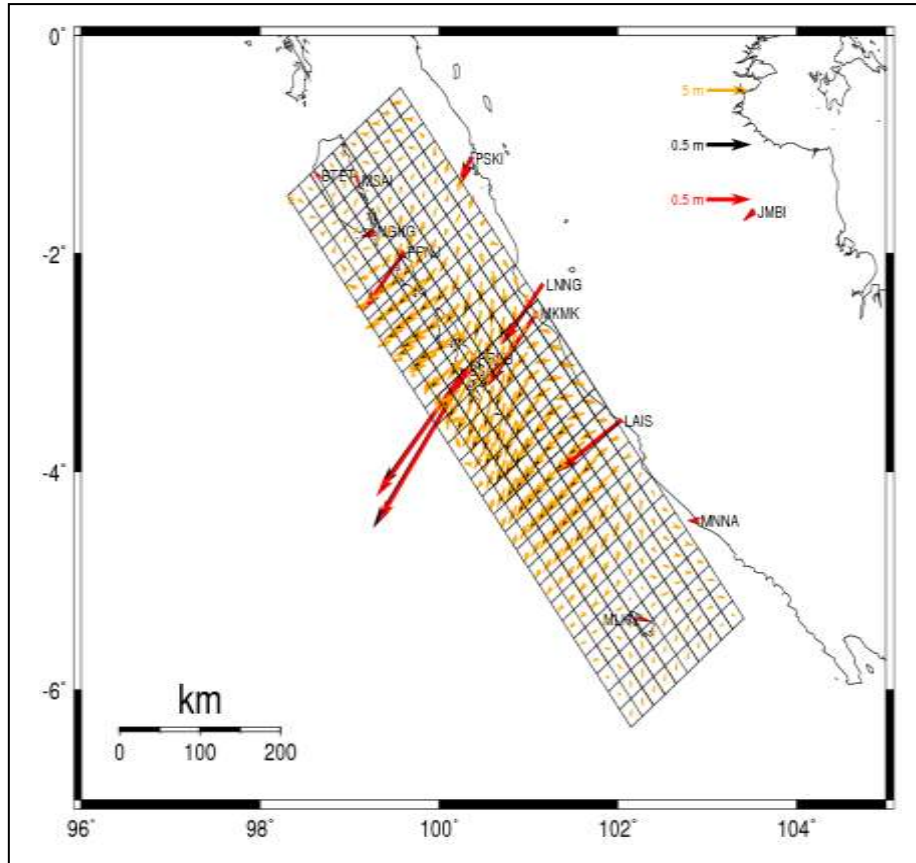


**Figure 7** Slip distribution as a result of the inversion of SuGAR data for 30 x 10 discrete field units with weight combination 3 (black vectors depict the vector of each point's displacement using SuGAR data, red vectors are the model's displacement vectors; orange vectors are the slip yielded from the inversion of discrete-field data).



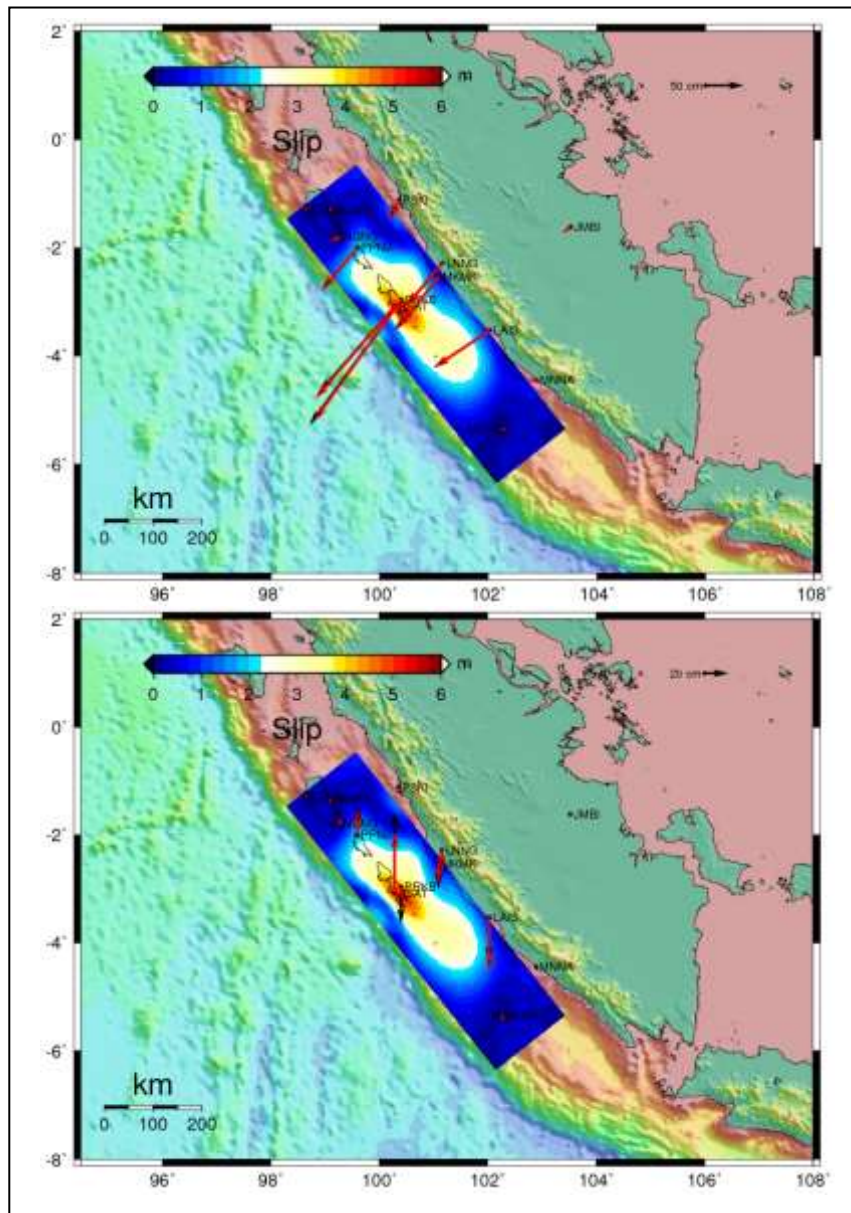


**Figure 8** Contour of the slip distribution resulting from the inversion of SuGAR data for  $30 \times 10$  discrete fields with weight combination 3 (the upper image is the horizontal component, the lower image is the vertical component, the black vectors are the vectors of each point's displacement using SuGAR data, the red vectors are the model's displacements vectors).

## 7 Seismic Moment and RMS Estimation

Seismic moment was calculated using the assumed value of coefficient  $\mu$  (coefficient of rigidity) =  $4 \times 10^{10} \text{ N.m}^{-2}$  (table 2). Moment magnitude was calculated using the formula of Kanamori and Anderson [16].

**Table 2** Seismic moment and moment magnitude (Mw).

	Moment (N.m)	Mw
<b>30x10 discrete field units weight 1</b>	7.452E+21	8.5
<b>30x10 discrete field units weight 2</b>	6.501E+21	8.5
<b>30x10 discrete field units weight 3</b>	7.140E+21	8.5
<b>USGS [7]</b>	5.050E+21	8.4 (8.5*)
<b>Gusman, <i>et al.</i> [8]</b>	3.800E+21	8.3
<b>Global CMT Solution [10]</b>	6.71E+21**)	8.5**)
* ) results from seismic data		
** ) results from seismic data		

The slip distributions resulting from the inversion were used to calculate the displacements in order to obtain the model displacement vectors. The RMS values of the observed and calculated displacement vectors are shown in Table 3.

**Table 3** RMS values of observed and calculated displacement vectors.

Type of discrete field unit	RMS (meter)		
	RMS	RMS horizontal	RMS vertical
<b>30x10 discrete field units weight 1</b>	0.109	0.061	0.173
<b>30x10 discrete field units weight 2</b>	0.106	0.063	0.165
<b>30x10 discrete field units weight 3</b>	0.061	0.028	0.100

RMS values for the horizontal component ranged from 28 mm to 63 mm, while the vertical component varied between 100 mm and 173 mm. The smallest RMS value in the inversion was the one resulting from the use of weight combination 3.

## 8 Closing Remarks

The slip patterns resulting from the inversion calculation are very similar for every weight combination, i.e. the maximum slip values are concentrated around PRKB station (Pagai Island) and BSAT station (Pagai Island), and they decrease toward the edges of the earthquake field. In addition, the values of dip-

slip direction tend to be more dominant and the slip direction inclines toward the trench. This is consistent with the mechanism of the Bengkulu earthquake, with its dominant dip-slip.

The three weight combinations used to calculate the inversion give a seismic moment value of , which is similar to the value calculated using the USGS teleseismic data. Weight combination 3 yields the lowest values for the RMS of the residual vectors of the GPS data and the model. Therefore, weight combination 3 is considered to give the optimal slip distribution.

The maximum slip values according to this paper are 3.75 m, 3.95 m and 5.12 m, while the maximum slip values resulting from the USGS study, Gusman, *et al.* [8] and Ambikapathy, *et al.* [9] are 4 m, ~6 m and 7 m, respectively. The location of maximum slip in these studies is consistent, i.e. around Pagai Island. Also, the slip direction vectors resulting from this paper, USGS and Ambikapathy, *et al.* [9] are similar, i.e. tending toward the trench.

## References

- [1] USGS, [http://neic.usgs.gov/neis/eq\\_depot/2007/eq\\_070912\\_hear/neic\\_hear\\_1.html](http://neic.usgs.gov/neis/eq_depot/2007/eq_070912_hear/neic_hear_1.html) (12 May 2010).
- [2] Meilano, I., Abidin, H.Z., Andreas, H., Gumilar, I., Sarsito, D., Hanifa, R., Rino, Harjono, H., Kato, T., Kimata, F. & Fukuda Y., *Slip Rate Estimation of the Lembang Fault West Java from Geodetic Observation*, Journal of Disaster Research, **7**(1), 2012.
- [3] Prawirodirdjo, L., Bock, Y., McCaffrey, R., Genrich, J., Calais, E., Stevens, C., Puntodewo, S.S.O., Subarya, C., Rais, J., Zwick, P. & Fauzi., *Geodetic Observations of Interseismic Strain Segmentation at the Sumatra Subduction Zone*, Geophys. Res. Lett., **24**(21), pp. 2601-2604, November 1, 1997.
- [4] Abidin, H.Z., Andreas, H., Kato, T., Ito, T., Meilano, I., Kimata, F., Natawidjaja D.H., Harjono, H., *Crustal Deformation Studies in Java (Indonesia) Using GPS*, Journal of Earthquake and Tsunami, **3**(2), (2009) 77–88.
- [5] Okada, Y., *Surface Deformation Due to Shear and Tensile Faults in A Half Space*, Bull. Seism. Soc. Am., **75**, pp. 1135-1154, 1985.
- [6] Du, Y., Aydin A. & Segall, P., *Comparison of Various Inversion Techniques as Applied to the Determination of a Geophysical Deformation Model for the 1983 Borah Peak Earthquake*, Bull. Seism. Soc. Am., **82**(4), pp. 1840-1866, 1992.
- [7] USGS, [http://earthquake.usgs.gov/earthquakes/eqinthenews/2007/us2007\\_hear/finite\\_fault.php](http://earthquake.usgs.gov/earthquakes/eqinthenews/2007/us2007_hear/finite_fault.php) (12 May 2010).

- [8] Gusman, A., Latief, H., Pandoe, W. & Tanaka, Y., *Source Model of the 2007 Bengkulu Earthquake Determined from Tsunami Waveforms and InSAR Data*, Symposium on Estimating the Recurrence Interval and Behavior of Tsunamis in the Indian Ocean via a Survey of Tsunami-related Sedimentation, Tsukuba, 2009.
- [9] Ambikapathy, A., Catherine, J.K., Gahalaut, V.K., Narsaiah, M., Bansal, A. & Mahesh, P., *The 2007 Bengkulu Earthquake, Its Rupture Model and Implications for Seismic Hazard*, J. Earth Syst. Sci., **119**(4), pp. 553-560, Indian Academy of Sciences, 2010.
- [10] Global CMT, <http://www.globalcmt.org/> (3 August 2010).
- [11] Menke, W., *Geophysical Data Analysis: Discrete Inverse Theory*, Academic Press. San Diego, California, 1989.
- [12] Lawson, C.L. & Hanson, D.J., *Solving Least Squares Problems*, Prentice-Hall, Englewood Cliffs, New Jersey, 1974.
- [13] Segall, P., *Earthquake and Volcano Deformation*, Princeton University Press. New Jersey, 2010.
- [14] Hugentobler, U., Dach, R. & Fridez, P. (Eds.), *Bernese GPS Software*, Version 5.0, University of Bern, 2004.
- [15] Bos, M.S. & Scherneck, H.G., *Free Ocean Tide Loading Provider*, 2004, <http://www.oso.chalmers.se/loading/> (5 August 2010).
- [16] Kanamori H. & Anderson, D.L., *Theoretical Basis of Some Empirical Relations In Seismology*, Bull. Seismol, Soc. Am., **65**, pp. 1073-95, 1975.